

High Impedance Fault Modeling Based on Statistical Data

W. C. Santos, N. S. D. Brito, B. A. Souza, F. A. Pereira

Abstract--The implementation of fast and reliable techniques able to detect and locate high impedance faults (HIF) is becoming increasingly an issue of interest to electric utilities. In order to test and validate those techniques, simulated signals are vital. However, the simulated fault voltages and currents must have complex characteristics, such as intermittency, transients, buildup, shoulder, nonlinearity, and asymmetry, which can completely change with the contact surface. In some cases, HIF may have significant differences even within the same contact surface. In order to evaluate the characteristics of HIF 129 experiments were staged at Energisa, a Brazilian electrical power distribution utility, taking into account contact surfaces, such as: asphalt, grass, crushed stone, sand, pavement, and local soil. The characteristics of each record were evaluated and a statistical analysis was performed. In this work variations on intermittency and shoulder are included in database records. Each record, even though belonging to the same contact surface database, have distinct characteristics.

Keywords: ATP, fault diagnose, fault modeling, high impedance fault, MODELS.

I. INTRODUCTION

AMONG the many disturbances that the electric power systems are subject, faults (short circuits) are undoubtedly the most worrisome. In the case of distribution systems, a special class of faults called high impedance faults (HIFs) is cause for concern, especially in overhead distribution networks. A HIF occurs when an energized conductor of the primary network makes an electrical contact with a surface of high resistive value, resulting in overcurrents insufficient to sensitize the protection system [1], [2]. As a result, the fault is not cleared, exposing the population to the risk of electric shock and compromising system equipment integrity.

In this context, the implementation of fast and reliable techniques able to detect and locate HIF is becoming increasingly an issue of interest to electric utilities. In order to test and validate those techniques, simulated signals are vital. However, the simulated fault voltages and currents must have complex characteristics, such as intermittency, transients, buildup, shoulder, nonlinearity, and asymmetry, which can

completely change with the contact surface [3]. In some cases, HIF may have significant differences even within the same contact surface. Features like moisture, the way in which the energized conductor contacts the surface of high impedance, the rise of new conduction paths in the soil during the failure, among others, may cause different waveforms of voltages and fault currents [4].

This work presents the development of a HIF model based on real data and their statistical variations. The Electrical Systems Group of Federal University of Campina Grande has been working with HIF since 2008 with research ranging from experiments and modeling [1], [4], [5] to the detection and location [2], [6] of these disorders. Several experiments were staged at Energisa, a Brazilian electrical power distribution utility, taking into account dry and wet contact surfaces: grass, crushed stone, sand, pavement, and local soil. In total 129 oscillographic records were obtained. Each contact surface had its own behavior, but in many cases, there was considerable variation between records of the same surface, mainly for the characteristics of intermittency and shoulder. In this sense, the characteristics of intermittency and shoulder of each record were evaluated and a statistical analysis was performed to describe the amount of cycles (repetitions) and the duration of these features in the records obtained from field trials.

The application of statistical survey was conducted in model applying the mean and standard deviation for the duration and number of repetitions of shoulder and intermittency. The effective contribution of this work is the inclusion of variations on intermittency and shoulder in records created in databases. Each record, even though belonging to the same contact surface database, have distinct characteristics.

II. HIF FEATURES

A HIF occurs when an energized conductor of the primary network makes an electrical contact with a surface of high resistive value, resulting in an overcurrent insufficient to sensitize the conventional protection system. Consequently, the fault is not cleared, exposing the population to the risk of electric shock as well as compromising the integrity of the system equipment and of private devices.

According to [7], HIFs generally cause the appearance of electric arcs, leading to some fault current peculiarities that are described next:

- *Asymmetry*: The fault current has different absolute values for positive and negative half cycle;
- *Nonlinearity*: The voltage-current characteristic curve is

This work was supported by the Brazilian National Research Council (CNPq) and by the Brazilian Coordination for Improvement of Higher Education Personnel (CAPES).

W. C. Santos is a Ph. D. student at Federal University of Campina Grande, Brazil (e-mail of corresponding author: wellinsilvio.santos@ee.ufcg.edu.br).

N. S. Brito and B. A. Souza are with the Department of Electrical Engineering, Federal University of Campina Grande, Brazil (e-mail: nubia@dee.ufcg.edu.br; benemar@dee.ufcg.edu.br).

nonlinear;

- *Buildup*: The current magnitude increases gradually to its maximum value;
- *Shoulder*: Buildup is ceased for a few cycles;
- *Intermittence*: Some cycles in which the energized wire interrupts the contact with the soil.

Fig. 1 shows an example of a HIF field test record. On the one hand, nonlinearities and asymmetries occur in the whole signal, on the other hand, the intermittence shows up at around 0.3 s, whereas both buildup and shoulder occur around 0.55 s. HIFs also generate electromagnetic transients between 2 and 10 kHz due to the intermittent permanence of the wire on the contact surface [8]. Such high frequency components may be extracted through suitable signal processing techniques and then used to detect HIFs instead of conventional overcurrent-based techniques, guaranteeing more reliable fault detections.

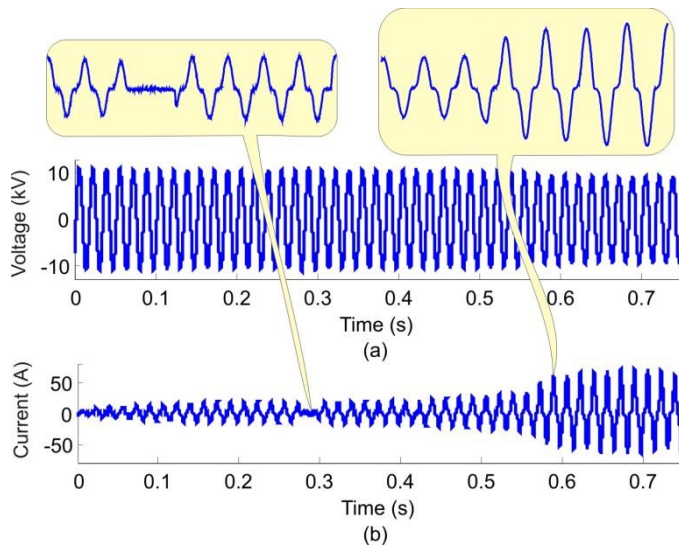


Fig. 1. An actual HIF oscillographic record: (a) voltage; (b) current.

III. HIF TESTS

Staged HIF tests are unusual in the daily of utilities. In these tests some risks are involved, which if not prevented may cause problems, such as damage to the electrical system, especially to sensitive equipment, unexpected shutdowns, risk of death in humans and animals through step voltages and direct contact with the energized conductors, and fire hazard.

In order to avoid that a large number of costumers being affected by an unexpected shutdown, the workgroup decided to perform the tests in a 13.8 kV rural feeder localized at Boa Vista town, Brazil.

Representatives from each group visited the city and chose as the location for the tests a farm 15 km away from the substation (Fig. 2). The farm has enough space to prepare experiments and to shelter the teams during the test implementation, safely. Using the utility engineering software, the current levels of solid short circuits were obtained. Thus, currents at test location can reach up to 475, 410 and 404 amperes for three-phase, biphasic and mono-phase faults,

respectively.

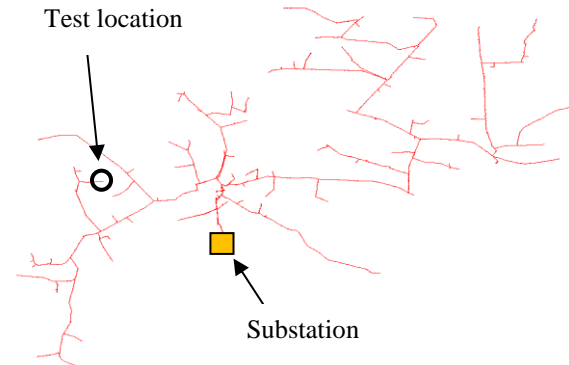


Fig. 2. The chosen feeder of Boa Vista substation.

Three measurement poles were chosen along the feeder (Fig. 3). Data obtained from the fault location pole (1) were used to support computational simulations. Data obtained from the remote poles (3 and 4) were used to evaluate the HIF transient diminishing and estimate more precisely the range of diagnosis methods. This work used fault location data.

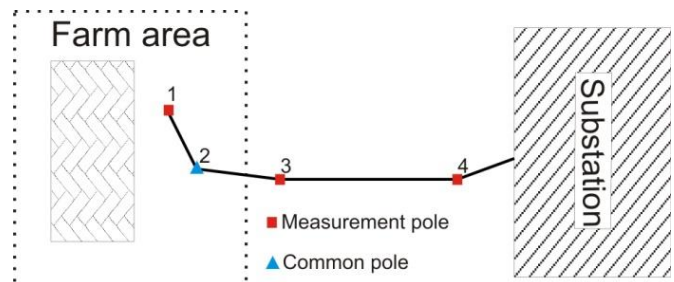


Fig. 3. Top view of the experimental setup.

On measurement poles, current and potential transformers were installed. During the tests, Digital Fault Recorders (DFR) were installed on them in order to capture the oscillographic data. The pole distances between substation and farm area are shown in Table 1.

TABLE 1
MEASUREMENT POLES DISTANCES

Distance to	Pole 1	Pole 3	Pole 4
Test location in km	0	1.0	11.0
Substation in km	15.0	14.0	4.0

The structure built for the tests followed the similar idea of tests described in [1]. They were done on six different kinds of contact surfaces: grass, gravel, pavement, asphalt, sand, and local soil (Fig. 4). After being tested dry, the surfaces were wet and the tests were repeated.

A two-meter transition pole was placed between the common pole and the fault point, in order to install potential and current transformers. A ladder and an insulating rod were put near the common pole in order to change fuses when necessary. A 13.8 kV conductor coming from the common pole was connected to the transition pole and to an insulating rod. An insulating scaffold was placed in order to enable a technician to manipulate the energized conductor safely (Fig. 5). The testing area was isolated and signaled.



Fig. 4. The structure built in order to execute the staged fault testing.

For data obtainment, a DFR with 15360 Hz sampling frequency was installed at the fault point and configured in order to enable the measurement, recording, and viewing of the events to be generated in the tests. Another DFR was installed at each remote monitoring place at a time. In this way, each experiment had two records, one at de fault location and the other at the remote place. DFRs were configured for 30 seconds recording. Both fault and remote location groups had radios to communicate during the tests.



Fig. 5. A technician on the insulating scaffold manipulating an energized conductor.

IV. HIF MODELING

The goal of HIF models is to allow tools and components available in computer simulators to be able to develop routines that generate records with similar characteristics from those of a real disorder. These simulated records are important because of the possibility of new detection and location methods to be tested with them, besides the fact that actual HIF data are difficult to obtain. Thus, the closer the simulated records are from real records, the more reliable the conclusions drawn in

diagnostic methods based on them.

In this sense, the 129 registers from HIF tests were analyzed. It was observed that the characteristics of intermittence and shoulder had considerable variation even among the same contact surface records.

A. Statistical Analysis

In records of the same surfaces were observed variations in the characteristics of shoulder and flashing. Figs. 6 and 7 show cases where these differences appear in records on the pavement and gravel, respectively.

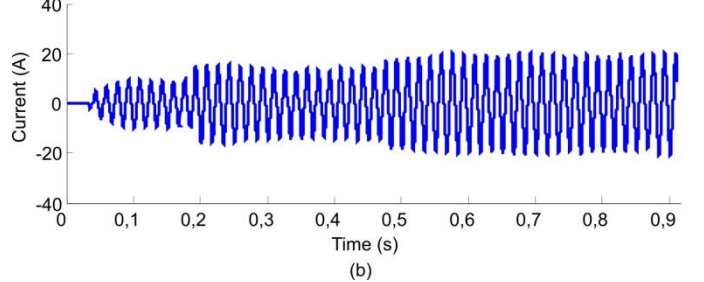
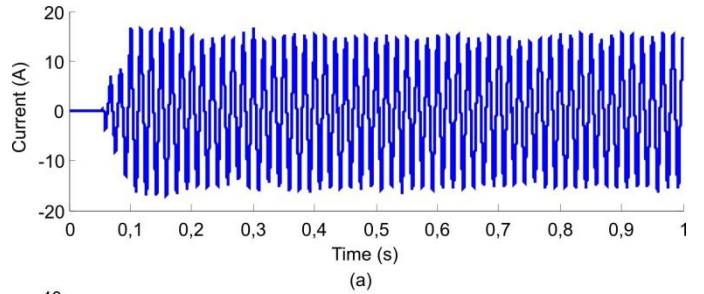


Fig. 6. Records on the pavement: (a) without the appearance of shoulder cycles; (b) with two shoulder cycles.

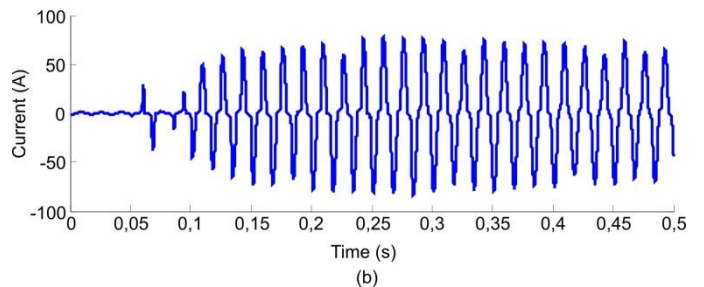
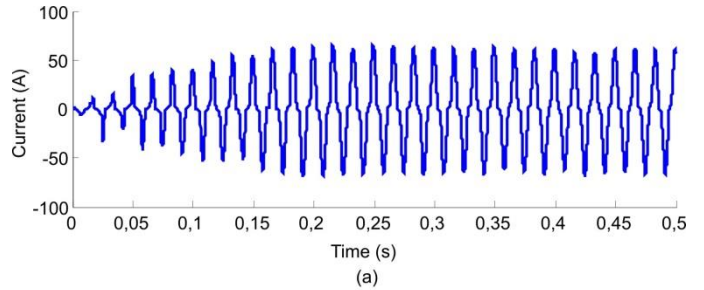


Fig. 7. Records on the gravel: (a) without the appearance of intermittence cycles; (b) with one intermittence cycle.

Tables II and III respectively show the amount of cycles (repetitions) and the duration of intermittence and shoulder characteristics in the records obtained from field tests. Each contact surface had their own behavior, but in many cases there were considerable variation between records of the same

surface.

TABLE II
INTERMITTENCE STATISTICAL ANALYSIS

Contact Surface	Cycles		Duration	
	Average	Standard Deviation	Average	Standard Deviation
Grass	0.00	0.00	0.00	0.00
Gravel	1.14	1.07	3.09	2.83
Pavement	0.80	0.63	4.43	2.30
Asphalt	1.17	0.75	4.40	1.52
Sand	0.30	0.48	1.67	0.58
Local soil	0.60	0.89	1.50	0.71

TABLE III
SHOULDER STATISTICAL ANALYSIS

Contact Surface	Cycles		Duration	
	Average	Standard Deviation	Average	Standard Deviation
Grass	0.92	0.86	5.50	2.00
Gravel	0.63	0.74	2.75	0.50
Pavement	0.85	0.69	3.78	1.20
Asphalt	1.23	0.83	2.82	0.75
Sand	1.00	0.82	4.44	1.33
Local soil	1.50	0.71	5.30	1.41

The effective contribution of this work is the inclusion of the variations of intermittence and shoulder characteristics in the records created in databases. Each record, even if belonging to the same contact surface and with the same simulation variables, will have different characteristics.

B. HIF Model

In order to choose a HIF model, the characteristics of the phenomenon must be represented adequately. The state of the art shows that most researches are based on models that use diodes [9] or association of nonlinear impedances [10]. Although these methods represent the nonlinear and the asymmetry characteristics of HIFs well, they do not embrace the other characteristics, such as buildup, shoulder, and intermittence.

This work adapted a model proposed by [11], which simulates the characteristics of nonlinearity, asymmetry, buildup, and shoulder by employing two time-varying resistances (TVRs) controlled by TACS in ATP. In this model, resistance R_1 represents the characteristics of nonlinearity and asymmetry (providing the same characteristics at every cycle of the signal), while resistance R_2 represents the characteristics of buildup and shoulder (just influencing at the beginning of the signal).

As this model does not consider intermittence, a simple TACS-controlled switch (STCS) was added to it. This switch will eliminate the HIF for a few cycles and then will close again. According to the oscillographic data analysis, in these cases, the fault current is interrupted some cycles after the fault initiation, generally, in a zero voltage passage. Some cycles later, there is the arc re-ignition, generally, in a peak voltage passage. A common switch was used in order to isolate the portion of the feeder downstream from the failure

point. Fig. 8 depicts the model adopted for the HIF.

The voltage and current waveforms of the staged faults were used. In order to fit R_1 value only one cycle of the steady-state in HIF condition is taken into account. In addition, to simplify the HIF model implementation in ATP, only 32 points of the selected cycle were considered. The original signal have 256 points/cycle (sampling frequency of 15360 Hz).

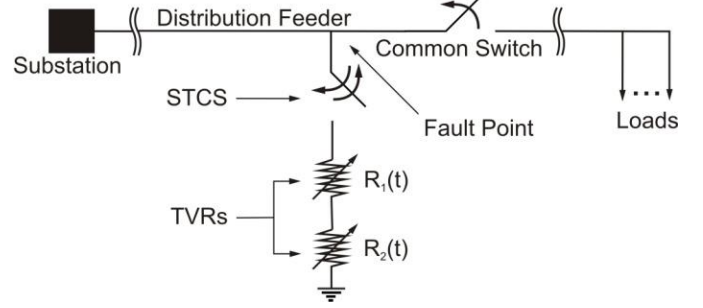


Fig. 8. Model adopted for the HIF.

The current corresponded to the faulted voltage is computed as follows

$$i(t) = \begin{cases} i_n + \frac{i_{n+1} - i_n}{v_{n+1} - v_n} \times \Delta v, & \text{if } v_n < v(t) < v_{n+1} \\ i_n, & \text{if } v(t) = v_n \end{cases} \quad (1)$$

where:

$\Delta v = v(t) - v_n$ in Volt (V);

i_n = Current at sample n in Ampere (A);

v_n = Voltage at sample n in Volt (V).

The resistance R_1 can be estimated by the rate between voltage and current at a steady-state fault cycle. Buildup and shoulder are regarding to fault current magnitude variation. As consequence, resistance R_2 is calculated considering only the maximum absolute value of voltage and current (Fig. 9).

Considering τ_k as the instant which the absolute value of current and voltage reach their maximum values for the k th half cycle after HIF, the total resistance $R(\tau_k)$ is obtained by dividing $v(\tau_k)$ by $i(\tau_k)$. Since the characteristics of nonlinearity and asymmetry are nearly constant during the HIF, $R_1(\tau_k)$ is approximately constant too. Thus, $R_2(\tau_k)$ is obtained by subtracting $R_1(\tau_k)$ from $R(\tau_k)$.

In order to simulate the characteristics related to the amplitude of the HIF current in their initial cycles, two curves [12] can be considered (Fig. 10). The first curve (Fig. 10a) in addition to considering the effect of buildup, also takes into account constant intervals in the growth of current (shoulder). At this point is where the contributions actually appear in relation to other models [1], [4]. Instead of using polynomial functions to accomplish the alignment of points $R_2(\tau_k)$ [1], [4], an exponential function was used. This choice was made in order to make possible the insertion of shoulder small variations among the various records of a database. Such variation was observed in the records obtained in field tests, but was not considered by models previously created [1], [4].

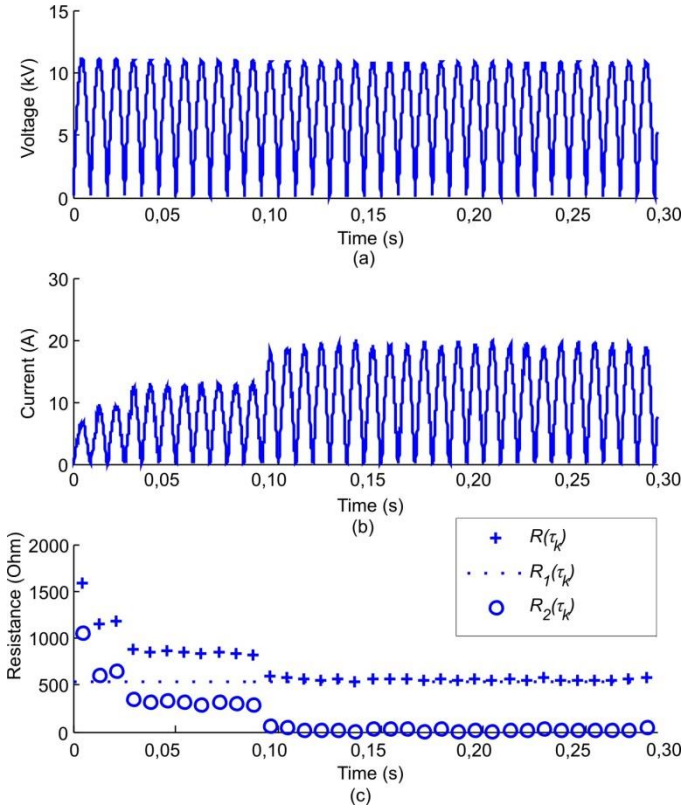


Fig. 9. R_2 calculation process on the pavement: (a) Absolute value of HIF voltage; (b) Absolute value of HIF current; (c) resistance value versus time.

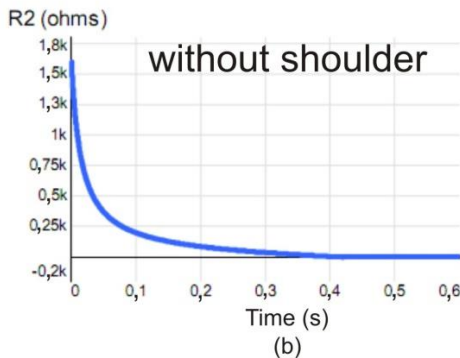
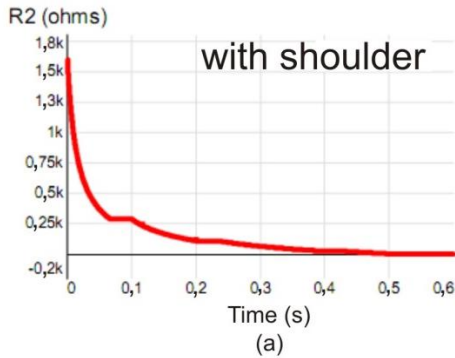


Fig. 10. Resistance R_2 as a function of time: (a) considering shoulder; (b) disregarding shoulder [12].

Finally, $R_2(t)$ is obtained by the $R_2(\tau_k)$ linearization using the method of least squares. For instance, the obtained resistance on local soil was

$$R_2(t) = 817.4e^{-13.4t}. \quad (2)$$

In order to consider shoulder in $R_2(t)$, breaks of constancy in the exponential decay were performed in each of the records in the database created. The duration and frequency of these intervals followed the statistical analysis presented in Table III. Similarly, intermittence was simulated based on the data of Table II. Fig. 11 depicts a simulated HIF record.

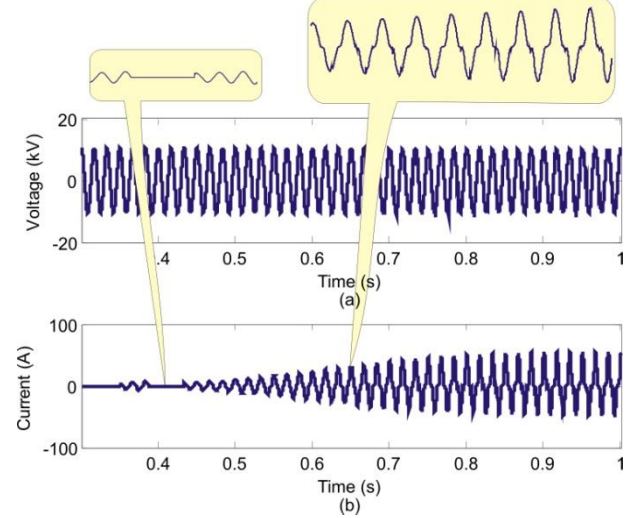


Fig. 11. A simulated HIF oscillographic record: (a) voltage; (b) current.

V. DATABASE BUILDING

The building process of the database was divided into three steps: pilot system modeling, the choice of simulation variables, and database building itself.

A. Simulated Feeder

A 13.8 kV distribution feeder where HIF tests were performed was chosen to be modeled. To make the modeling possible, the utility provided data about the chosen feeder, such as: power of transformers, wire and poles characteristics, and distances between transformers.

Simulations were performed in ATP considering:

- Non-transposed three-phase lines at distributed and constant parameters with the frequency.
- Stretches consisting of only one type of cable: cable 4 American Wire Gauge (AWG).
- Loads of near points along the feeder, grouped on an only bus, resulting in a feeder with 90 buses (Fig. 12).
- Skin effect factor of 0.33 for the cables.
- Resistivity of the ground (350 $\Omega \cdot m$).
- Model of constant impedance for the loads.
- Loads modeled as parallel RL circuits connected between each phase of each bus and the ground.
- Average power factor of 0.955.

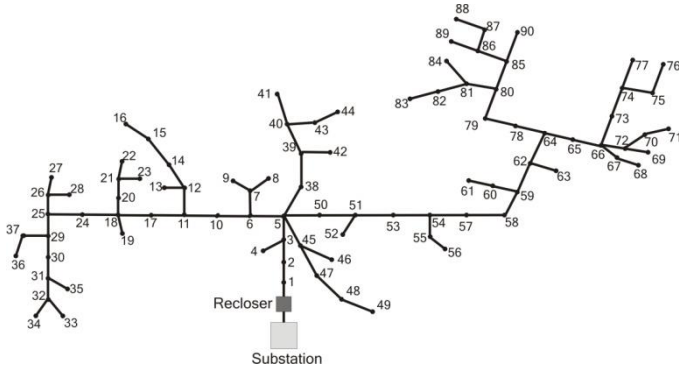


Fig. 12. Modeled 90 bus feeder.

B. Simulation Variables

In order to validate fault location and detection tools several situations of faults should be evaluated on a system.

In this work the used simulation variables were: fault location, contact surface, and load conditions. Only faults between one phase and ground were simulated.

The considered load conditions varied between 25 to 100% by 25% of installed capacity. Nine among ninety buses were chosen as fault locations. The total period of each simulation was one second, with 0.333 second as pre-fault time. A summary of the simulation variables is presented in Table IV.

TABLE IV
SIMULATION VARIABLES

Simulation variables	Specification
Fault type	AN
Load condition (%)	25, 50, 75, 100
Fault location (Bus)	10, 23, 30, 44, 49, 56, 63, 68, 90
Contact surface	Grass, gravel, pavement, asphalt, sand, and local soil

C. HIF Database

The database building process was divided into three stages: creation of the various fault ATP files, compilation of each file, and conversion of ATP output files into IEEE-COMTRADE format.

The function \$PARAMETER of ATP was used in order to facilitate the changes in the database building process. This function receives the constants of each simulation variables cases. Each simulation variable was placed in a known line and was changed by the database building routine, creating the schemes of faults.

To convert ATP output into IEEE-COMTRADE format a C++ program was implemented. ATP output is similar to IEEE-COMTRADE, but its content is real and must be

integer. Thus, the C++ program converts real numbers of the ATP output into integer numbers.

A Matlab® routine was implemented to manage the database building process. This routine was responsible for:

- Modifying ATP files (.atp) and creating the desired variable combinations;
- Creating and running a batch file (.bat) containing execution commands to run ATP files, the convertor C++ program, and erase non-interesting files, sequentially;
- Creating CFG files (.cfg) that together to the convertor C++ program output shape the IEEE-COMTRADE format.

Statistical analyzes were used for records with the same simulation variables had different behaviors of intermittence and shoulder. These differences must comply with average and standard deviation characteristics of each contact surface.

A specific nomenclature was given for each case. From this name it's possible to know all the conditions where that case occurred. For example:

DFR(S)_fAN_BUS10_SAN_C25_rep1.

This the first case of a HIF recorded by a DFR in the substation, between phase "A" and ground, occurring at bus 10, on sand, with 25% of total load.

The routine in Matlab® was responsible for creating the schemes of faults in ATP and executing each case. A summary of the construction of the database is presented in Fig. 13.

The database was divided into six parts, each one receiving the name of the contact surface used in its simulation.

Table V provides the size of each database and the total number of different schemes of faults.

TABLE V
DATABASE NUMBERS

Database	Contact Surface	Number of records
I	Grass	36
II	Gravel	36
III	Pavement	36
IV	Asphalt	36
V	Sand	36
VI	Local soil	36
Total		216

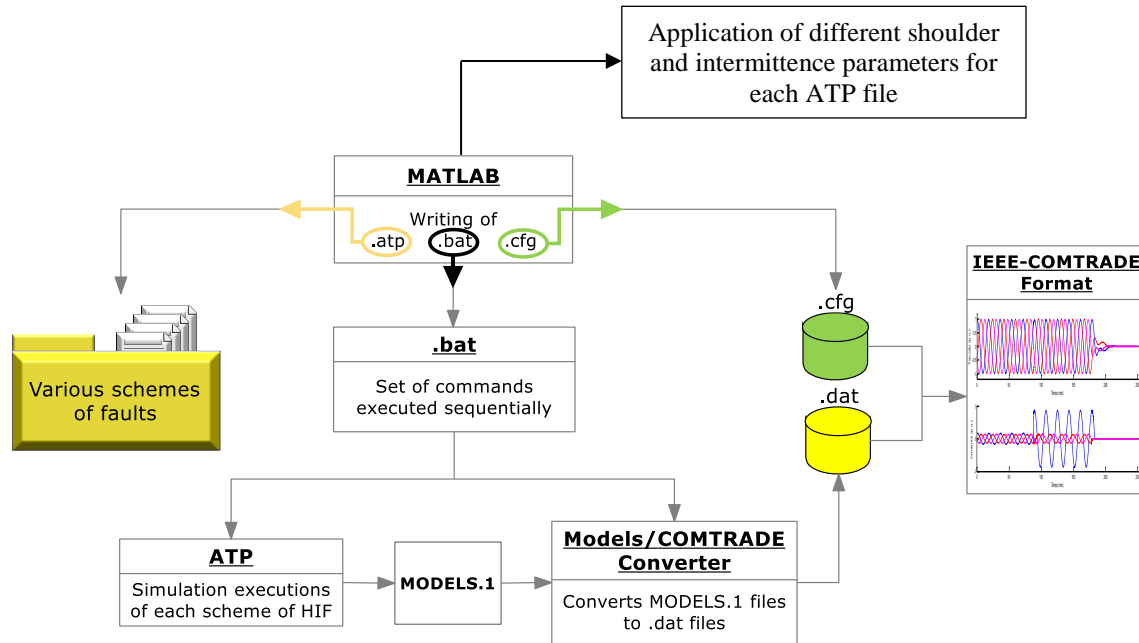


Fig. 13. Process of database building.

Fig. 14 shows simulated HIF current on pavement. Although belonging to the same database, the records have differences in the appearance of the shoulder and intermittence features.

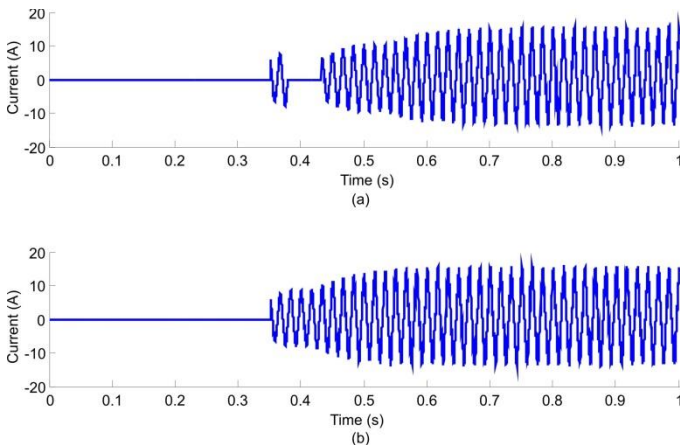


Fig. 14. HIF currents on the pavement: (a) with one intermittence and shoulder cycles; (b) no intermittence cycle and one shoulder cycle.

VI. CONCLUSIONS

Computational tools based on computational intelligence are of the utmost versatility and wide use in the diagnosis of faults field. However, the need to databases that are representative to the studied phenomenon makes it difficult to use, since a large amount of data to have a reliable final result is required.

HIF field tests were performed and allowed a better understanding of the characteristics of HIF. These characteristics varied in incidence and intensity among the different contact surfaces tested. Even among the records obtained in the same contact surface considerable differences

in the characteristics of intermittence and shoulder were observed.

From a statistical analysis of data obtained in field tests was possible to generate records with same simulation variables but with different times of incidence of intermittence and shoulder. The proposed HIF database enables development of new diagnostic methods in addition to the performance evaluation of existing ones.

VII. REFERENCES

- [1] W. C. Santos, F. Costa, J. Silva, G. Lira, B. Souza, N. Brito, and M. Paes Jr., "Automatic building of a simulated high impedance fault database," in *2010 IEEE/PES Transmission and Distribution Conference and Exposition: Latin America (T&D-LA)*, nov. 2010, pp. 550–554.
- [2] J. A. C. B. Silva, F. B. Costa, W. C. Santos, G. R. S. Lira, W. L. A. Neves, B. A. Souza, N. S. D. Brito, and M. R. C. Paes Jr., "High impedance fault location - case study with developed models," in *21st International Conference on Electricity Distribution (CIRED 2011)*, Frankfurt, jun. 2011.
- [3] Jeerings D. I.; Linders J. R., "Ground resistance-revisited," *IEEE Trans. Power Delivery*, vol. 4, no. 2, pp. 949–956, Apr 1989.
- [4] W. C. Santos, B. A. Souza, N. S. D. Brito, F. B. Costa, M. R. C. Paes Jr., "High Impedance Faults: From Field Tests to Modeling", in *Journal of Control, Automation and Electrical Systems*, vol 24, no 6, pp. 885-896, September 2013.
- [5] W. C. Santos, G. R. S. Lira, F. B. Costa, J. A. C. B. Silva, B. A. Souza, N. S. D. Brito, M. R. C. Paes Jr., "Staged-Fault Testing for High Impedance Fault Data Collection and Simulation Support", in *17th International Symposium on High Voltage Engineering*, 2011, Hannover, Germany.
- [6] W. C. Santos, F. V. Lopes, N. S. D. Brito, B. A. Souza, D. Fernandes Jr., W. L. A. Neves, "High Impedance Fault Detection and Location Based on Electromagnetic Transient Analysis", in *International Conference on Power Systems Transients (IPST2013)* in Vancouver, Canada July 18-20, 2013.
- [7] EPRI, "EPRI Report: Detection of Arcing Faults on Distribution Feeders," Palo Alto, Tech. Rep., 1982.
- [8] A.-R. Sedighi, M.-R. Haghifam, O. Malik, and M.-H. Ghassemian, "High impedance fault detection based on wavelet transform and statistical pattern recognition," *Power Delivery, IEEE Transactions on*, vol. 20, no. 4, pp. 2414–2421, oct. 2005.

- [9] A. E. Emanuel; E. M. Gulachenski; D. Cyganxki, A. J. Orr; S. Shiller. "High impedance fault arcing on sandy soil in 15kV distribution feeders: contributions to the evaluation of the low frequency spectrum," *IEEE Trans. Power Delivery*, vol.5, n. 2, pp. 676-686, April 1990.
- [10] D. C. YU; S. H. KHAN, "An adaptive high and low impedance fault detection method," *IEEE Trans. Power Delivery*, vol. 9, n. 4, pp. 1812–1821, October 1994.
- [11] S. R. Nam, J. K. Park, Y. C. Kang, T. H. Kim. "A modeling method of a high impedance fault a distribution system using two series time-varying resistances in EMTP", in *IEEE PES Summer Meeting 2001*, vol. 2, pp. 1175-1180.
- [12] F. M. Uriarte, "Modeling, Detection, And Localization of High-Impedance Faults In Low-Voltage Distribution Feeders". Master's thesis. Faculty of the Virginia Tech Polytechnic Institute and State University. 2003.